Title

A framework for modeling and analysis of dynamical properties of spiking neurons

ISBN

9781479932726

Authors

Phillips, S

Sanfelice, RG

Publication Date

2014

DOI

10.1109/ACC.2014.6859494

Peer reviewed

A Framework for Modeling and Analysis of Dynamical Properties of Spiking Neurons

Sean Phillips and Ricardo G. Sanfelice

***Abstract*— A hybrid systems framework for modeling and analysis of robust stability of spiking neurons is proposed. The framework is developed for a population of n interconnected neurons. Several well-known neuron models are studied within the framework, including both excitatory and inhibitory simplified Hodgkin-Huxley, Hopf, and SNIPER models. For each model, we characterize the sets that the solutions to each system converge to. Using Lyapunov stability tools for hybrid systems, the stability properties for each case are established. An external stimuli is introduced to the simplified Hodgkin-Huxley model to achieve a global asymptotic stability property. Due to the regularity properties of the data of the hybrid models considered, the asserted stability properties are robust to small perturbations. Simulations provide insight on the results and the capabilities of the proposed framework.**

I. Introduction

Neuron models are commonly regarded as a typical non-smooth/impulsive system. The literature proposes many different frameworks for analysis of such systems, including compartmental models [1], phase plane models [2], [3], integrate-and-fire and impulsive differential equations [3], [4], [5], and large populations of interconnected neurons (neuron population models) [6], [3], [7]. Furthermore, being a natural process, these interconnections between neurons are inherently noisy [8], [9]. Unfortunately, there is a distinct lack of systematic methods for analysis of robustness of such interconnections.

Building from recent results on robustness of stability of hybrid systems and motivated by the lack of tools for analysis of robustness in neurons, we propose a unifying framework to model and analyze spiking neuron models. Due to the impulsive nature of spiking neurons, hybrid systems provide a very promising platform for their study. In this paper, we model spiking neurons as hybrid dynamical systems for which asymptotic stability and robustness can be systematically studied. The proposed hybrid framework captures the continuous evolution of the phase dynamics of the neurons as well as their spiking/discontinuous behavior due to internal and external stimuli. The study of the asymptotic stability properties of these systems is performed using the tools in [10], [11].

This paper is organized as follows. In Section II we introduce the general framework and specific models under consideration then, in Section III-A, we characterize the sets where solutions converge for several well-known neuron models. In particular, within the proposed framework, we consider the simplified Hodgkin-Huxley model [3], [12]; an inhibitory version of the Hodgkin-Huxley model; a "saddle-node on a periodic orbit" model, known as the SNIPER model [2]; and the Hopf model proposed in [13]. In Sections III-B - III-E, details of the stability analysis for the case of two neurons and for each one of the phase response curves associated with the models just listed are given. In addition to the cases without external stimuli, in Section IV, we design a external stimuli for the simplified Hodgkin-Huxley model that guarantees a global stability property. Simulations that validate our results are also included. In Section V, we compare our results to those established in the literature.

S. Phillips and R. G. Sanfelice are with the Department of Aerospace and Mechanical Engineering, University of Arizona 1130 N. Mountain Ave, AZ 85721. Email: sap86@email.arizona.edu,sricardo@u.arizona.edu.
This research has been partially supported by the National Science Foundation under CAREER Grant no. ECS-1150306 and by the Air Force Office of Scientific Research under Grant no. FA9550-12-1-0366.

Notation: $\mathbb{R}$ denotes the real numbers space. $\mathbb{R}^n$ denotes the n-dimensional Euclidean space. $\mathbb{N}$ denotes the natural numbers including zero. Given an interval $\mathcal{S} = [0, t]$ and $n \in \mathbb{N} \setminus \{0\}$, $\mathcal{S}^n$ is the cartesian product of the interval, i.e., $[0, t]^3 = [0, t] \times [0, t] \times [0, t]$. The Euclidean distance from $x \in \mathbb{R}^n$ to a set $S \subset \mathbb{R}^n$ is denoted by $d(x, S)$. A column vector of N ones is denoted by $\mathbf{1}$. The graph of a set-valued mapping $F : \mathbb{R}^n \rightrightarrows \mathbb{R}^n$ is $\text{gph}(F) = \{(x, y) : x \in \mathbb{R}^n, y \in F(x)\}$. A class-$\mathcal{KL}$ function $\beta : \mathbb{R}_{\geq 0} \times \mathbb{R}_{\geq 0} \to \mathbb{R}_{\geq 0}$ is nondecreasing in its first argument and nonincreasing in its second argument, furthermore, $\lim_{r \to 0^+} \beta(r, s) = 0$ for each $s \in \mathbb{R}_{\geq 0}$ and $\lim_{s \to 0^-} \beta(r, s) = 0$ for each $r \in \mathbb{R}_{\geq 0}$.

II. A Framework For Analysis for Spiking Neurons

A. Introduction to Neuron Models

A single neuron can be expressed by the general N-order, conductance based model given generically by

$$\dot{x} = I(x) + I^g(x, t), \tag{1}$$

where $x = (v, w) \in \mathbb{R}^N$, $v \in \mathbb{R}$ is the voltage difference across the membrane, w is the $(N-1)$-dimensional vector comprising the gating variables, $I(x)$ is the baseline vector field, and $I^g(x, t)$ is the stimulus effect, see [3], [2], [14].

Using a change in parameters and an approximation (seen in [3], [6], [15]), the evolution of the phase of the single neuron can be captured by the first order differential equation

$$\frac{d\theta}{dt} = \omega + z(\theta)I(t), \tag{2}$$

with the natural frequency $\omega = \frac{2\pi}{T} > 0$. The period T is the time between the spiking and reset events of the singular neuron model in (1), while z and is the phase response curve (PRC) characterizing the neurons sensitivity to the

given stimulus. PRCs can be calculated from experimental, numerical, and analytical studies [14], [16].

B. Hybrid Modeling

Due to its impulsive nature, the neuron model presented in Section II-A can be modeled as a hybrid system. Specifically, the phase angle θ will flow continuously according to the natural frequency and jump when the neuron spiking condition is met. Utilizing the formulation of hybrid systems in [10], [11], we propose a framework for modeling neurons given by

$$\mathcal{H} \; : \quad x \in \mathbb{R}^n \quad \begin{cases} \dot{\theta} = f(\theta) & \theta \in C \\ \theta^+ \in G(\theta) & \theta \in D \end{cases}, \qquad (3)$$

where $\theta = [\theta_1, \ldots, \theta_n]^\top \in [0, 2\pi]^n$ is the phase of n neurons, with $\theta_i \in [0, 2\pi]$ being the phase of the i-th neuron. The continuous dynamics of each neuron are represented by a natural frequency ω_i, i.e., $\dot{\theta}_i = \omega_i$, which leads to $f(\theta) := [\omega_1, \ldots, \omega_n]^\top$. From the neuron model (2), the natural frequency is related to the spiking period T, in that, when the phase angle reaches 2π, the neuron activates the PRC. Then, the flow set is given by $C := [0, 2\pi]^n$ while jumps occur when θ is in the jump set given by $D := \{\theta \in C : \exists \; i \text{ s.t. } \theta_i = 2\pi\}$. Lastly, as previously described, each neuron jumps impulsively once any i-th neuron reaches a full period, i.e., $\theta_i = 2\pi$ from some i. At such an event, the neuron resets itself to zero and induces a reset on all other neurons by instantaneously changing their phase angles according to the PRC, namely, θ_i is reset to $\gamma(\theta_i) = \theta_i + hz(\theta_i)$, where $h > 0$ is the synapse coupling strength. In this way, the jump map is given as $G(\theta) = [g(\gamma(\theta_i)), \ldots, g(\gamma(\theta_n))]^\top + G^u(\theta)$, where

$$g(s) = \begin{cases} 0 & \text{if } s > 2\pi \text{ or } s \leq 0 \\ \{0, s\} & \text{if } s = 2\pi \\ s & \text{if } s < 2\pi \text{ and } s > 0 \end{cases} \qquad (4)$$

and $G^u : \mathbb{R}^n \rightrightarrows \mathbb{R}^n$ is a set-valued map representing an external stimuli. Note that g is set valued when the state is such that, after the jump, it is exactly 2π. By defining it set valued, (rather than just discontinuous) robust stability results for hybrid systems can be applied.

Solutions to the hybrid system $\mathcal{H}$ evolve continuously (flow) and/or discretely (jump) depending on the continuous and discrete dynamics, and the sets where those dynamics apply. As in [11], we treat the number of jumps as an independent variable j and the amount of time of flows by the independent variable t. Then, solutions θ to $\mathcal{H}$ are given by *hybrid arcs* parameterized by (t, j), which take values on the *hybrid time domain* dom θ: see [10], [11] for details.[1]

This general framework for neurons can be used to study the stability of different PRCs (synchronizing and desynchronizing) as well as their robustness. In our study of dynamical properties of neurons, we consider the following PRCs:

1) Simplified Hodgkin-Huxley model: $z(\theta) = -\sin(\theta)$;
2) Inhibited simplified Hodgkin-Huxley model: $z(\theta) = \sin(\theta)$;
3) SNIPER model: $z(\theta) = 1 - \cos(\theta)$;
4) Hopf model: $z(\theta) = -\sin(\theta - \theta_0)$.

C. Basic Properties of $\mathcal{H}$

To apply the stability analysis tools for hybrid systems outlined in [11], the hybrid system (3) must satisfy certain conditions, namely, the *hybrid basic conditions*. These conditions are as follows:

A1) C and D are closed sets in $\mathbb{R}^n$.
A2) $f : \mathbb{R}^n \to \mathbb{R}^n$ is continuous on C.
A3) $G : \mathbb{R}^n \rightrightarrows \mathbb{R}^n$ is an outer semicontinuous[2] set-valued mapping, locally bounded on D, and such that $G(\theta)$ is nonempty for each $\theta \in D$.

Lemma 2.1: Let z be continuous and G^u be outer semicontinuous. Then, the hybrid system $\mathcal{H}$ satisfies the hybrid basic conditions.

With these conditions being satisfied, asymptotic stability of a compact set automatically implies that it is robust to vanishing state disturbances as well as other types of small perturbations [11].

III. Stability Analysis of Synchronization and Desynchronization with Zero Inputs

A. Proposed Approach

Our goal is to characterize the set of points, denoted $\mathcal{A}$, that, for each of the considered PRC cases, is asymptotically stable. Asymptotic stability for hybrid systems is defined as the property of a set being both *stable* and *attractive* [10], [11]. These properties are defined as follows:

Definition 3.1: (stability) A compact set $\mathcal{A} \subset \mathbb{R}^n$ is said to be

- *stable* if for each $\varepsilon > 0$ there exists $\delta > 0$ such that each solution x with $|x(0,0)|_{\mathcal{A}} \leq \delta$ satisfies $|x(t,j)|_{\mathcal{A}} \leq \varepsilon$ for all $(t, j) \in$ dom x;
- *attractive* if there exists $\mu > 0$ such that every solution x with $|x(0,0)|_{\mathcal{A}} \leq \mu$ is complete and satisfies $\lim_{(t,j)\in \text{dom } x, t+j\to\infty} |x(t,j)|_{\mathcal{A}} = 0$;
- *asymptotically stable* if stable and attractive.

The basin of attraction for asymptotic stability, denoted $\mathcal{B}_{\mathcal{A}}$, is the set of points where the attractivity property holds. It excludes points from where solutions may never converge to $\mathcal{A}$. We denote this set as $\mathcal{X}$. Since, in this paper, we will analyze neuron model with PRCs, and each case is inherently different, we will characterize this specific set for each case.

For example, for the study of synchronization in neuron models, the set $\mathcal{A}$ for $n = 2$ is given by the points in the jump set and away from $\mathcal{A}$ where $|\theta_1 - \theta_2|$ remains constant before and after the jump. Namely, it is defined by the values of θ satisfying

$$|\theta_1 - \theta_2| = |\theta_1^+ - \theta_2^+|. \qquad (5)$$

[1] A solution θ is said to be *nontrivial* if dom θ contains at least one point different from $(0, 0)$, *maximal* if there does not exist a solution θ' such that θ is a truncation of θ' to some proper subset of dom θ', *complete* if dom θ is unbounded, and *Zeno* if it is complete but the projection of dom θ onto $\mathbb{R}_{\geq 0}$ is bounded.

[2] A set-valued mapping $G : \mathbb{R}^N \rightrightarrows \mathbb{R}^N$ is *outer semicontinuous* if its graph is closed [11, Lemma 5.10], see, e.g., [17].

To solve (5), let $h_1 = h_2 = h$, $\theta \in D \setminus \mathcal{A}$ with $\theta_1 = 2\pi$ and $\theta_2 = \theta^*$ such that $\theta^* + hz(\theta^*) \in (0, 2\pi)$. After the jump, $\theta_1^+ = 0$ and $\theta_2^+ = \theta^* + hz(\theta^*)$. Then

$$|2\pi - \theta^*| = |0 - (\theta^* + hz(\theta^*))|$$
$$\implies 2\pi - 2\theta^* = hz(\theta^*). \tag{6}$$

Similar results hold if $\theta_1 = \theta^*$ and $\theta_2 = 2\pi$. Then, the set $\mathcal{X}$ is given by $\mathcal{X} := \{\theta \in [0, 2\pi]^2 : |\theta_1 - \theta_2| = 2\pi - \theta^*, 2\pi - 2\theta^* = hz(\theta^*)\}$.

The approach in this paper is to employ Lyapunov stability results for hybrid systems in [10], [11] to establish that the set $\mathcal{A}$ is asymptotically stable for the hybrid system $\mathcal{H}$. To establish this property, a definition of a Lyapunov function candidate for hybrid systems and sufficient conditions for asymptotic stability are needed.

Definition 3.2: (Lyapunov candidate) Given the hybrid system $\mathcal{H}$ with state (C, f, D, G) and a compact set $\mathcal{A} \subset \mathbb{R}^n$, the function $V : \text{dom } V \to \mathbb{R}$ is a Lyapunov function candidate for $(\mathcal{H}, \mathcal{A})$ if

i) V is continuous and nonnegative on $(C \cup D) \setminus \mathcal{A} \subset \text{dom } V$;
ii) V is continuously differentiable on an open set $\mathcal{O}$ satisfying $C \setminus \mathcal{A} \subset \mathcal{O} \subset \text{dom } V$;
iii) $\lim_{x \to \mathcal{A}, x \in \text{dom } V \cap (C \cup D)} V(x) = 0$.

Sufficient conditions for asymptotic stability in terms of Lyapunov functions can be found in [11], [10].

B. Simplified Hodgkin-Huxley (HH) Model ($n = 2$)

From [3], the simplified Hodgkin-Huxley model has a PRC function z given by $z(\theta) = -\sin(\theta)$. The associated neuron model with $n = 2$, $\omega_1 = \omega_2 = \omega > 0$, $h \in (0, \pi)$ and no external stimuli ($G^u = 0$) can be written in the framework (3) with data

$$\mathcal{H}_{HH} := \begin{cases} C := [0, 2\pi] \times [0, 2\pi] \\ f(\theta) = [\omega, \omega]^\top \qquad \forall \theta \in C \\ D := \{(\theta_1, \theta_2) \in C : \exists i \in \{1, 2\} \text{ s.t. } \theta_i = 2\pi\} \\ G(\theta) = [g(\gamma(\theta_1)), g(\gamma(\theta_2))]^\top \qquad \forall \theta \in D \end{cases} \tag{7}$$

and the PRC given by $z(\theta) = -\sin(\theta)$. The function g in the jump map G is defined as in (4) with $\gamma(\theta_i) = \theta_i - h\sin(\theta_i)$, for each $i \in \{1, 2\}$. Note that when $\theta \in D$ is such that $\theta_i + h\sin(\theta_i) = 2\pi$, the function $g(\theta_i + h\sin(\theta_i))$ is set valued.

The simplified Hodgkin-Huxley model is known to synchronize the phases of the neurons, i.e., $|\theta_1 - \theta_2|$ approaches zero. For this system, the set to be stabilized is denoted $\mathcal{A}_{HH}$. It is defined as $\mathcal{A}_{HH} = \{(\theta_1, \theta_2) \in [0, 2\pi]^2 : |\theta_1 - \theta_2| = 0\}$ and represents a synchronization condition. To determine the set of points ($\mathcal{X}$ in Section III) from where solutions to $\mathcal{H}_{HH}$ never converge to $\mathcal{A}_{HH}$, we follow the computation to arrive to (6). With $z(\theta) = -\sin(\theta)$, (6) becomes $2\pi = 2\theta^* - h\sin\theta^*$. The only solution to this expression is $\theta^* = \pi$, for any $h \in (0, \pi)$. Then, the set $\mathcal{X}_{HH}$ for $\mathcal{H}_{HH}$ is defined by $\mathcal{X}_{HH} := \{(\theta_1, \theta_2) : |\theta_1 - \theta_2| = \pi\}$.

Now, to establish that $\mathcal{A}_{HH}$ is asymptotically stable, consider the function defined on C as in (7) as

$$V_{HH}(\theta) = \min\{|\theta_1 - \theta_2|, 2\pi - |\theta_1 - \theta_2|\}. \tag{8}$$

This function satisfies the conditions for it to be a candidate Lyapunov function on $(C \cup D) \setminus \mathcal{X}_{HH}$ (see Definition 3.2). In fact, it is continuous everywhere, continuously differentiable away from $\mathcal{X}_{HH}$, positive for all $\theta \in (C \cup D) \setminus (\mathcal{A}_{HH} \cup \mathcal{X}_{HH})$, and $V_{HH}(\theta) = 0$ for all $\theta \in \mathcal{A}_{HH}$. In fact, we have the following result.

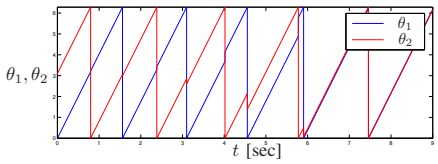

(a) A time trajectory to the hybrid system $\mathcal{H}_{HH}$

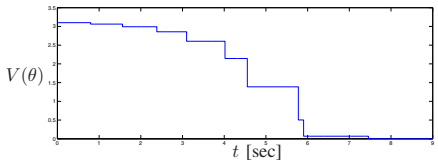

(b) The corresponding Lyapunov function along the solution to $\mathcal{H}_{HH}$.

Fig. 1. A solution θ to the simplified Hodgkin-Huxley hybrid system $\mathcal{H}_{HH}$ with $\theta(0, 0) = [0, 3.1]^\top$. Note that solutions become synchronized $(\theta_1(t, j) = \theta_2(t, j))$ and $V(\theta(t, j)) = 0$ at $(t, j) = (7.5, 9)$.

Lemma 3.3: The function V_{HH} in (8) is a Lyapunov function candidate for $\mathcal{H}_{HH}$ on $\{\theta \in [0, 2\pi]^2 : V(\theta) < \pi\}$.

With this function, it can be shown that for every point in the flow set we have $\dot{V} = 0$ while, for points $\theta \in D \setminus (\mathcal{X}_{HH} \cup \mathcal{A}_{HH})$, we have that $V(G(\theta)) - V(\theta) < 0$. These properties lead to the following result.

Theorem 3.4: The hybrid system (7) with $z(\theta) = -\sin(\theta)$ has the set $\mathcal{A}_{HH}$ asymptotically stable with the basin of attraction given by $(C \cup D) \setminus \mathcal{X}_{HH}$.

Figure 1 is a solution to $\mathcal{H}_{HH}$ with $h = 0.9$ and initial condition $\theta(0, 0) = [0, 3.1]^\top$; this solution starts just outside of the set $\mathcal{X}_{HH}$.

C. Inhibited Simplified Hodgkin-Huxley (IHH) Model ($n = 2$)

In this section, we consider the inhibited simplified Hodgkin-Huxley model. The PRC for this case is given by $z(\theta) = \sin(\theta)$. The positive sign on the sine function of the PRC has an inhibitory effect (compared to the excitatory response of the case in Section III-B): after every jump, the distance between the phases grows until they are a maximum distance apart. The resulting hybrid system is denoted as $\mathcal{H}_{IHH}$, which has the same data as in (7) except that $\gamma(\theta_i) = \theta_i + h\sin(\theta_i)$ with $h \in (0, \pi)$.

The set $\mathcal{X}_{IHH}$ is given by the points θ such that $\theta_1 = \theta_2$ and the points from where there could be a jump to $\theta_1 = \theta_2$. This set is given by $\mathcal{X}_{IHH} := \{\theta \in C : \theta_1 = \theta_2\} \cup \{(0, 2\pi), (0, 2\pi)\}$.

We define the set $\mathcal{A}$ for $\mathcal{H}_{IHH}$ as $\mathcal{A}_{IHH} := \ell_1 \cup \ell_2$ where $\ell_1 := \{\theta \in \mathbb{R}^2 : \theta = \widetilde{\theta}_1 + \mathbf{1}s, s \in \mathbb{R}\}$ and $\ell_2 := \{\theta \in \mathbb{R}^2 :$

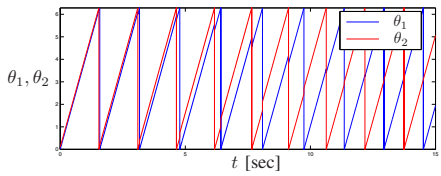

(a) A solution to the hybrid system $\mathcal{H}_{IHH}$.

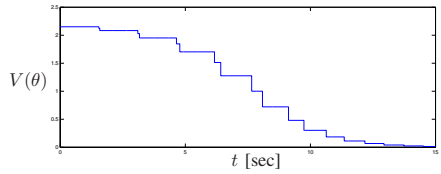

(b) The corresponding Lyapunov function along the solution to $\mathcal{H}_{IHH}$.

Fig. 2. A solution θ to the simplified Inverse Hodgkin-Huxley hybrid system $\mathcal{H}_{IHH}$ with $\theta(0,0) = [0, 0.1]^\top$.

$\theta = \widetilde{\theta}_2 + \mathbf{1}s, s \in \mathbb{R}\}$ with $\widetilde{\theta}_1 = \begin{bmatrix} 2\pi \\ \pi \end{bmatrix}$ and $\widetilde{\theta}_2 = \begin{bmatrix} \pi \\ 2\pi \end{bmatrix}$.

The sets ℓ_i represent lines in $\mathbb{R}^2$. Following [18], a Lyapunov function V_{IHH} can be defined as the distance from θ to the set $\mathcal{A}_{IHH}$. More specifically, $V_{IHH}(\theta) = d(\theta, \mathcal{A}_{IHH})$ for each $\theta \in [0, 2\pi]^2 \setminus \mathcal{X}_{IHH}$. The expression of the function V_{IHH} can be further reduced to the minimum distance to each set ℓ_i, namely $V_{IHH}(\theta) = \min\{d(\theta, \ell_1), d(\theta, \ell_2)\}$ while the distance $d(\theta, \ell_i)$ can be rewritten as $d(\theta, \ell_i) = \left|(\theta - \widetilde{\theta}_i) - \frac{1}{2}((\theta - \widetilde{\theta}_i)^\top \mathbf{1})\mathbf{1}\right|$, where $\widetilde{\theta}_i$ is defined for each ℓ_i as above. We have the following result.

Lemma 3.5: The function V_{IHH} is a Lyapunov function candidate for $\mathcal{H}_{IHH}$ on $\{\theta \in [0, 2\pi]^2 : V(\theta) < \frac{\pi}{\sqrt{2}}\}$.

Similar to $\mathcal{H}_{HH}$, we can use a Lyapunov stability argument to show the stability of $\mathcal{A}_{IHH}$ for $\mathcal{H}_{IHH}$. The proof of this theorem follows closely that of the one for $\mathcal{H}_{HH}$, in that, during flows we have that $\dot{V} = 0$ everywhere, during jumps the difference is strictly decreasing, i.e., $V(G(\theta)) - V(\theta) < 0$ for each $\theta \in D \setminus (\mathcal{X}_{IHH} \cup \mathcal{A}_{IHH})$.

Theorem 3.6: The hybrid system $\mathcal{H}_{IHH}$ with the PRC $z(\theta) = \sin(\theta)$ has the set $\mathcal{A}_{IHH}$ asymptotically stable with basin of attraction $(C \cup D) \setminus \mathcal{X}_{IHH}$.

Figure 2 shows a solution to $\mathcal{H}_{IHH}$ with $h = 1$ and $\theta(0,0) = [0, 0.1]^\top$, and the values of the corresponding Lyapunov function along the solutions.

D. SNIPER (S) Model ($n = 2$)

The SNIPER model has the PRC given by $z(\theta) = (1 - \cos(\theta))$. The resulting hybrid system with this PRC is denoted as $\mathcal{H}_S$. It has the same data as in (7) except that $\gamma(\theta_i) = \theta_i + h(1 - \cos(\theta_i))$ with $h > 0$. The solutions to the SNIPER system converge to the set

$$\mathcal{A}_S := \{(\theta_1, \theta_2) \in [0, 2\pi]^2 : |\theta_1 - \theta_2| = 0\} \tag{9}$$

which represents a synchronization condition. To determine the set of points ($\mathcal{X}$ in Section III) from where solutions to $\mathcal{H}_S$ never converge to $\mathcal{A}_S$, we follow the computation to (6), leading to

$$2\pi - 2\theta^* = h(1 - \cos(\theta^*)), \tag{10}$$

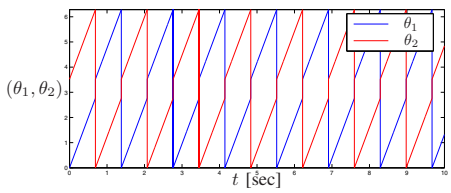

Fig. 3. A solution to $\mathcal{H}_S$ that never converges to $\mathcal{A}_S$ with $z(\theta) = 1 - \cos(\theta)$, $h = \pi/8$, and initial condition $\theta(0,0) = [0, 2\pi - \theta^*]^\top \in \mathcal{X}$.

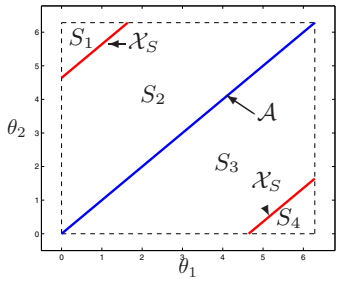

Fig. 4. The (θ_1, θ_2)-plane for the hybrid system $\mathcal{H}_S$ with $h = 2.67$.

which is an implicit expression on θ^*. As h increases, the right-hand side of (10) increases, and θ^* decreases. It follows that for $h > 0$, we have $\theta^* \in (0, \pi)$ and from (10), we obtain

$$\mathcal{X}_S := \{(\theta_1, \theta_2) \in [0, 2\pi]^2 : |\theta_1 - \theta_2| = 2\pi - \theta^*, \\ 2\pi - 2\theta^* = h(1 - \cos(\theta^*))\}.$$

Figure 3 shows a specific example of a solution to $\mathcal{H}_S$ with initial conditions $\theta(0,0) = [0, 3.52] \in \mathcal{X}$, and$h = \pi/8$.

To prove that $\mathcal{A}_S$ is asymptotically stable for $\mathcal{H}_S$, define the sets S_i as

$$S_1 = \{(\theta_1, \theta_2) \in [0, 2\pi]^2 : \theta_2 - \theta_1 > 2\pi - \theta^*\} \tag{11}$$
$$S_2 = \{(\theta_1, \theta_2) \in [0, 2\pi]^2 : 0 < \theta_2 - \theta_1 < 2\pi - \theta^*\} \tag{12}$$
$$S_3 = \{(\theta_1, \theta_2) \in [0, 2\pi]^2 : 0 < \theta_1 - \theta_2 < 2\pi - \theta^*\} \tag{13}$$
$$S_4 = \{(\theta_1, \theta_2) \in [0, 2\pi]^2 : \theta_1 - \theta_2 > 2\pi - \theta^*\}. \tag{14}$$

Figure 4 indicates each of the sets S_i, $\mathcal{A}_S$ and $\mathcal{X}_S$. Note that solutions to $\mathcal{H}_S$ that do not jump into $\mathcal{A}_S$ will jump between two S_i sets cyclicly. More precisely, we have the following result.

Lemma 3.7: Given the sets S_1, S_2, S_3, and S_4 in (11)-(14), if $\theta \in D \cap S_i$ and $\theta^+ \in G(\theta) \setminus (\mathcal{A}_S \cup \mathcal{X}_S)$, then:
(1) If $\theta \in S_1$, then $\theta^+ \in S_3$;
(2) If $\theta \in S_2$, then $\theta^+ \in S_4$;
(3) If $\theta \in S_3$, then $\theta^+ \in S_1$;
(4) If $\theta \in S_4$, then $\theta^+ \in S_2$.

Using a trajectory-based approach, we establish that $\mathcal{A}_S$ is attractive for $\mathcal{H}_S$.

Theorem 3.8: The hybrid system $\mathcal{H}_S$ with h satisfying $\cos(\theta_o - h(1 - \cos(\theta_o)) > \cos(\theta_o)$ for all $\theta_o \in (0, 2\pi - \theta^*)$, where θ^* satisfies (10), is such that the set $\mathcal{A}_S$ is attractive with basin of attraction $(C \cup D) \setminus \mathcal{X}_S$.

Remark 3.9: It can be determined numerically, that the condition in Theorem 3.8 holds for $h \in (0, 2.67)$. However, simulations show that solutions converge to $\mathcal{A}_S$ for larger values of h. In fact, since h proportionally affects the size of

the 'impulse,' the larger the value of h is the sooner solutions converge to $\mathcal{A}_S$.

E. Hopf (H) Model $(n = 2)$

The Hopf model has a PRC given by $z(\theta_i) = -\sin(\theta_i - \theta_0)$, where $\theta_0 \in (-\frac{\pi}{2}, \frac{\pi}{2})$ and $h \in (0, \pi)$, see, e.g., [19]. This PRC is similar to that of $\mathcal{H}_{HH}$ with a phase shift θ_0. The resulting hybrid system is denoted $\mathcal{H}_H$. It has the same data as in (7) except that $\gamma_i(\theta_i) = \theta_i + h\sin(\theta_i - \theta_0)$. For the range of $\theta_0 \in (-\frac{\pi}{2}, \frac{\pi}{2})$, solutions to this system approach the set $\mathcal{A}_H := \{(\theta_1, \theta_2) \in [0, 2\pi]^2 : |\theta_1 - \theta_2| = 0\}$. To determine the set from where solutions never converge to the set $\mathcal{A}_H$, namely to determine the set $\mathcal{X}_H$, from the computation in (6) with z given above, we obtain

$$2\pi - 2\theta^* = -h\sin(\theta^* - \theta_0) \tag{15}$$

which is an implicit equation parameterized by both h and θ_0. Then, the set $\mathcal{X}_H$ is defined by $\mathcal{X}_H := \{(\theta_1, \theta_2) : |\theta_1 - \theta_2| = 2\pi - \theta^*, 2\pi - 2\theta^* = -h\sin(\theta^* - \theta_0)\}$.

The function γ in the jump map can be rewritten as $\gamma(\theta_i) = \theta_i - h\sin(\theta_i)\cos(\theta_0) + h\cos(\theta_i)\sin(\theta_0)$. If we let $\rho(\theta_i, \theta_0) = h\cos(\theta_i)\sin(\theta_0)$ and $\tilde{h} = h\cos(\theta_0)$ then γ can be rewritten as

$$\gamma(\theta_i) = \theta_i - \tilde{h}\sin(\theta_i) + \rho(\theta_i, \theta_0) \tag{16}$$

We can now consider the offset θ_0 as a perturbation of the jump map in the simplified Hodgkin-Huxley model in Section III-B. This perturbation satisfies $|\rho(\theta_i, \theta_0)| \leq h|\sin(\theta_0)|$ for all $\theta_i \in [0, 2\pi]$. In this way, $\mathcal{H}_{HH}$ can be considered to be the unperturbed version of $\mathcal{H}_H$. Since $\mathcal{H}_{HH}$ satisfies the hybrid basic conditions from Lemma 2.1 and with $\mathcal{A}_{HH}$ being asymptotically stable for $\mathcal{H}_{HH}$, then using [11, Theorem 7.20], we have the following result.

Theorem 3.10: The hybrid system $\mathcal{H}_H$ has the set $\mathcal{A}_H$ practically asymptotically stable in the parameter $\theta_0 \in (\frac{-\pi}{2}, \frac{\pi}{2})$, i.e., for each $\varepsilon > 0$ there exists $\theta_0^* > 0$ and a $\mathcal{KL}$ function β such that, for each $|\theta_0| \in [0, \theta_0^*)$, every solution θ to $\mathcal{H}_H$ from $[0, 2\pi]^2 \setminus \mathcal{X}_H$ satisfies $|\theta(t, j)|_{\mathcal{A}_H} \leq \beta(|\theta(t, j)|_{\mathcal{A}_H}, t + j) + \varepsilon$ for all $(t, j) \in \text{dom } \theta$.

Figure 5 shows numerical results for large values of θ_0. The red regions correspond to points from where solutions converge to $\mathcal{A}_H$ (dashed cyan line), while the blue regions correspond to the points from where solutions "get stuck" due to the dynamics of the jump map. Moreover, the figure shows that as $|\theta_0|$ increases the blue regions get larger.

IV. Control of Neurons for Global Asymptotic Stability

This section illustrates the framework introduced in Section II on the $\mathcal{H}_{HH}$ model with an input given by an external stimuli. We design this input so that the almost global asymptotic stability property asserted by Theorem 3.4 becomes global.

Consider the hybrid system $\mathcal{H}_{HH}$. To guarantee that the set $\mathcal{X}_{HH}$ belongs to the basin of attraction, we define the external stimuli G^u that injects a small signal of value $\delta_i > 0$ around a small neighborhood of the set $\mathcal{X}_{HH}$.

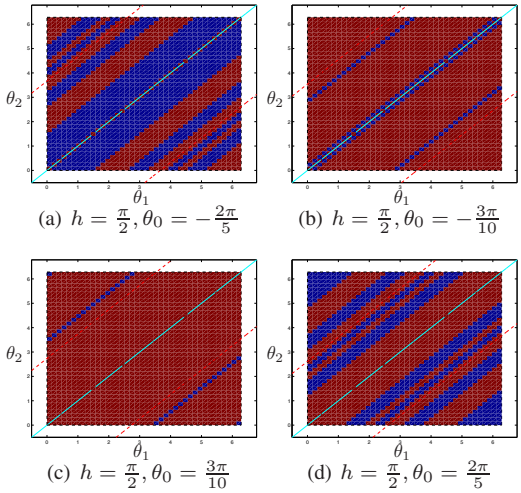

(a) $h = \frac{\pi}{2}, \theta_0 = -\frac{2\pi}{5}$ (b) $h = \frac{\pi}{2}, \theta_0 = -\frac{3\pi}{10}$

(c) $h = \frac{\pi}{2}, \theta_0 = \frac{3\pi}{10}$ (d) $h = \frac{\pi}{2}, \theta_0 = \frac{2\pi}{5}$

Fig. 5. Numerical solutions to $\mathcal{H}_H$ with initial conditions $\theta(0, 0) \in [0, 2\pi]^2$. The red regions correspond to the points that converge to $\mathcal{A}_H$ (dashed cyan) while the blue region corresponds to the points that "get stuck" near $\mathcal{A}_H$ due to the offset θ_0.

To this end, let $\lambda_i > 0$ and define the external input as $G^u(\theta) := [g^{u_1}(\theta), g^{u_2}(\theta)]^\top$, where

$$g^{u_i}(\theta) = \begin{cases} \delta_i & \text{if } \lambda_i < |\theta_1 - \theta_2| < \pi + \lambda_i, \\ \{0, \delta_i\} & \text{if } |\theta_1 - \theta_2| = \lambda_i \\ & \quad \text{or } |\theta_1 - \theta_2| = \pi + \lambda_i, \\ 0 & \text{if } |\theta_1 - \theta_2| < \lambda_i \\ & \quad \text{or } |\theta_1 - \theta_2| > \pi + \lambda_i. \end{cases} \tag{17}$$

The function g^{u_i} has a small value $\delta_i > 0$ on a band of size $\lambda_i > 0$ around the set $\mathcal{X}_{HH}$. These parameters need to be chosen so that $G(D) \subset [0, 2\pi]^2$. For example, if we choose $\lambda_i = \frac{\pi}{5}$ and $\delta_i = \frac{\pi}{6}$ the function $g_i^{u_i}$ leads to the bands around $|\theta_1 - \theta_2| = \pi$ seen in the middle graph in Figure 6. For the same parameters, Figure 6 suggests that for $\theta \in [0, 2\pi]^2$ the jump map is such that $G(\theta) \subset C \cup D$. Picking λ_i and δ_i to satisfy this property, it follows that by adding the set valued map G^u to the jump map of the hybrid system $\mathcal{H}_{HH}$, the jump map continues to satisfy the hybrid basic conditions. To show global asymptotic stability, we use the same Lyapunov function as in Theorem 3.4, namely $V(\theta) = \min\{|\theta_1 - \theta_2|, 2\pi - |\theta_1 - \theta_2|\}$.

Theorem 4.1: The hybrid system $\mathcal{H}_{HH}$ with outer semi-continuous $G^u(\theta) = [g^{u_1}(\theta), g^{u_2}(\theta)]^\top$ and g^{u_i} as in (17) such that $G(D) \subset [0, 2\pi]^2$, has $\mathcal{A}_{HH}$ globally asymptotically stable.

By adding the input term $g_i^{u_i}$, it follows from the proof of Theorem 3.4 and the results in [11] that we have global asymptotic stability of the set $\mathcal{A}_{HH}$ for the hybrid system in Section III-B.

V. Relationship with Previous Work

In Sections III-B and III-C, we consider the PRC given by $z(s) = -\sin(s)$ and $z(s) = \sin(s)$, respectively. These PRCs describe a simplified Hodgkin-Huxley model for different bifurcations points, as seen in [12]. As seen in Theorem 3.4 and Theorem 3.6, the hybrid system with negative PRC has solutions that converge to synchronization while the one with

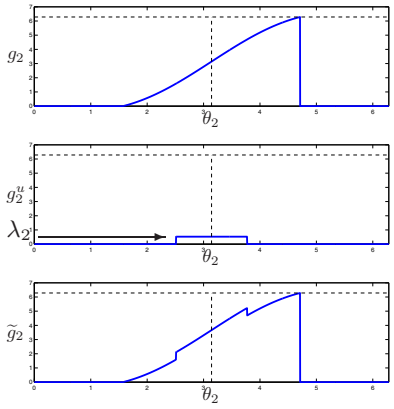

Fig. 6. An example of $\theta \in D$ when $\theta_1 = 2\pi$ and θ_2 is free with parameters given by $h = \pi/2$, $\gamma = \pi/5$, $\delta = \pi/6$.

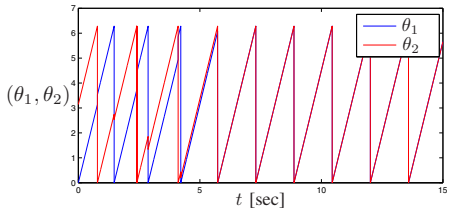

Fig. 7. A solution to $\mathcal{H}_{HH}$ with input injection initial condition $\theta(0,0) = [\pi, 2\pi]^\top$, and parameters $\delta = \pi/8$, $\gamma = 0.1$, $\omega = 4$, and $h = \pi/8$.

positive PRC has solutions that converge to desynchronization. These models follow from the simplification performed in [3]. On the other hand, Hodgkin and Huxley developed a complex model with multiple parameters corresponding to many bifurcations of solutions [12], each of which have been considered in vast detail in the literature [20], [21], while the desynchronizing bifurcation has been studied in [22].

The next model covered in this paper was the SNIPER model. This model is considered a type I neuron model (possessing a strictly positive PRC), which was initially derived in [2] for the $n = 2$ case and shown to synchronize under certain conditions on the speed of synapse. The phase response curve $z(\theta) = (1 - \cos(\theta))$ was indeed derived in [3], for which here we showed that this model does indeed synchronize the phase of each neuron asymptotically for almost every initial condition.

Lastly, we discussed the Hopf model. Its phase response curve was studied in [15], [19], [2]. In [3], the PRC is also dependent on a phase constant of the PRC. Here, we restrict this phase constant to a region about 0 so as to evaluate the stability of synchronization.

VI. Conclusion

A framework for modeling and analyzing groups of spiking neurons was introduced. Within the hybrid system framework, several well-known neuron models were studied, including the excitatory and inhibitory Hodgkin-Huxley model, the saddle-point node on a periodic orbit model (SNIPER), and the Hopf model. For each model, we characterized the sets to which their respective solutions converge. Using Lyapunov stability tools for hybrid systems, asymptotic stability properties were established for each system for the case of $n = 2$. The introduction of an external stimulation in the Hodgkin-Huxley neuron model is paramount in achieving global asymptotic stability. Since the data of the hybrid systems satisfies certain regularity properties, the stability of these systems is robust to small perturbations.

References

[1] J.M. Bower and D. Beeman. *The book of GENESIS: exploring realistic neural models with the GEneral NEural SImulation System*. TELOS, 1995.

[2] B. Ermentrout. Type i membranes, phase resetting curves, and synchrony. *Neural Comput*, 8:979–1001, 1995.

[3] E. E. Brown, J. Moehlis, and P. Holmes. On the phase reduction and response dynamics of neural oscillator populations. *Neural Comput.*, 16(4):673–715, April 2004.

[4] R. Stein. Some Models of Neuronal Variability. *Biophysical Journal*, 7(1):37–68, January 1967.

[5] C. Koch and I. Segev. *Methods in Neuronal Modeling: From Ions to Networks*. A Bradford book. MIT Press, 1998.

[6] Y. Kuramoto. Phase- and center-manifold reductions for large populations of coupled oscillators with application to non-locally coupled systems. *International Journal of Bifurcation and Chaos*, 07(04):789–805, 1997.

[7] W. Gerstner and W.M. Kistler. *Spiking Neuron Models: Single Neurons, Populations, Plasticity*. Cambridge University Press, 2002.

[8] D. H. Hubel and T. N. Wiesel. Ferrier lecture. Functional architecture of macaque monkey visual cortex. *Proceedings of the Royal Society of London. Series B, Containing papers of a Biological character. Royal Society (Great Britain)*, 198(1130):1–59, July 1977.

[9] W. R. Softky and C. Koch. The highly irregular firing of cortical cells is inconsistent with temporal integration of random EPSPs. *The Journal of Neuroscience*, 13(1):334–350, January 1993.

[10] R. Goebel, R.G. Sanfelice, and A.R. Teel. Hybrid dynamical systems. *IEEE Control Systems Magazine*, 29(2):28–93, April 2009.

[11] R. Goebel, R. G. Sanfelice, and A. R. Teel. *Hybrid Dynamical Systems: Modeling, Stability, and Robustness*. Princeton University Press, New Jersey, 2012.

[12] A. L. Hodgkin and A. F. Huxley. A quantitative description of membrane current and its application to conduction and excitation in nerve. *The Journal of physiology*, 117(4):500–544, August 1952.

[13] J.P. Keener and J. Sneyd. *Mathematical Physiology*. Interdisciplinary applied mathematics. U.S. Government Printing Office, 1998.

[14] A.T. Winfree. *The Geometry of Biological Time*. Interdisciplinary applied mathematics. U.S. Government Printing Office, 2001.

[15] J. Guckenheimer and P. Holmes. *Nonlinear Oscillations, Dynamical Systems, and Bifurcations of Vector Fields*. Number v. 42 in Applied Mathematical Sciences. Springer, 1983.

[16] L. Glass and M.C. MacKey. *From Clocks to Chaos: The Rhythms of Life*. Princeton Paperbacks. Mir, 1988.

[17] R.T. Rockafellar and R. J-B Wets. *Variational Analysis*. Springer, 1998.

[18] S. Phillips and R.G. Sanfelice. Results on the asymptotic stability properties of desynchronization in impulse-coupled oscillators. In *Proc. American Control Conference, 2013*, pages 3278–3283, June 2013.

[19] G. B. Ermentrout and N. Kopell. Frequency Plateaus in a Chain of Weakly Coupled Oscillators, I. *SIAM Journal on Mathematical Analysis*, 15(2):215–237, 1984.

[20] T. Ko and G. B. Ermentrout. Phase-response curves of coupled oscillators. *Phys. Rev. E*, 79(1):016211, Jan 2009.

[21] W. K. Luk and K. Aihara. Synchronization and sensitivity enhancement of the hodgkin-huxley neurons due to inhibitory inputs. *Biological Cybernetics*, 82(6):455–467, June 2000.

[22] S. K. Han, C. Kurrer, and Y. Kuramoto. Dephasing and bursting in coupled neural oscillators. *Phys. Rev. Lett.*, 75:3190–3193, October 1995.